



**HAL**  
open science

## **Trace Metals in Cloud Water Sampled at the Puy De Dôme Station**

Angelica Bianco, Mickaël Vaïtilingom, Maxime Bridoux, Nadine Chaumerliac,  
Jean-Marc Pichon, Jean-Luc Piro, Laurent Deguillaume

### ► **To cite this version:**

Angelica Bianco, Mickaël Vaïtilingom, Maxime Bridoux, Nadine Chaumerliac, Jean-Marc Pichon, et al.. Trace Metals in Cloud Water Sampled at the Puy De Dôme Station. *Atmosphere*, 2017, 8 (12), pp.225. <10.3390/atmos8110225>. <hal-01762390>

**HAL Id: hal-01762390**

**<https://uca.hal.science/hal-01762390v1>**

Submitted on 8 Jan 2019

**HAL** is a multi-disciplinary open access archive for the deposit and dissemination of scientific research documents, whether they are published or not. The documents may come from teaching and research institutions in France or abroad, or from public or private research centers.


L'archive ouverte pluridisciplinaire **HAL**, est destinée au dépôt et à la diffusion de documents scientifiques de niveau recherche, publiés ou non, émanant des établissements d'enseignement et de recherche français ou étrangers, des laboratoires publics ou privés.



Distributed under a Creative Commons CC BY 4.0 - Attribution - International License

Article

# Trace Metals in Cloud Water Sampled at the Puy De Dôme Station

Angelica Bianco <sup>1,2,\*</sup> , Mickaël Vaïtilingom <sup>1,2,†</sup>, Maxime Bridoux <sup>2</sup>, Nadine Chaumerliac <sup>1</sup>, Jean-Marc Pichon <sup>1</sup>, Jean-Luc Piro <sup>3</sup> and Laurent Deguillaume <sup>1,\*</sup>

<sup>1</sup> CNRS Laboratoire de Météorologie Physique, Université Clermont Auvergne, F-63000 Clermont-Ferrand, France; Mickael.Vaitilingom@univ-antilles.fr (M.V.); nadine.chaumerliac@uca.fr (N.C.); J.M.Pichon@opgc.fr (J.-M.P.)

<sup>2</sup> CEA, DAM, DIF, F-91297 Arpajon, France; maxime.bridoux@cea.fr

<sup>3</sup> CNRS Laboratoire Magma et Volcans, Université Clermont Auvergne, F-63000 Clermont-Ferrand, France; J.L.Piro@opgc.univ-bpclermont.fr

\* Correspondence: a.bianco@opgc.fr (A.B.); L.Deguillaume@opgc.fr (L.D.); Tel.: +334-73-40-5276 (A.B.); +334-73-40-7359 (L.D.)

† Current address: Laboratoire de Recherche en Géosciences et Energies, Département of Physics, Université des Antilles, 97110 Pointe-à-Pitre, France.

Received: 2 October 2017; Accepted: 14 November 2017; Published: 17 November 2017

**Abstract:** Concentrations of 33 metal elements were determined by ICP-MS (Inductively Coupled Plasma Mass Spectrometry) analysis for 24 cloud water samples (corresponding to 10 cloud events) collected at the puy de Dôme station. Clouds present contrasted chemical composition with mainly marine and continental characteristics; for some cloud events, a further anthropogenic source can be superimposed on the background level. In this context, measurements of trace metals may help to evaluate the impact of anthropogenic and natural sources on the cloud and to better discriminate the origin of the air masses. The metal concentrations in the samples are low (between 16.4  $\mu\text{g L}^{-1}$  and 1.46  $\text{mg L}^{-1}$ ). This could be explained by the remoteness of the puy de Dôme site from local sources. Trace metals are then used to confirm and refine a previous sample classification. A principal component analysis (PCA) using the pH value and the concentrations of  $\text{Cl}^-$ ,  $\text{NO}_3^-$ ,  $\text{SO}_4^{2-}$ ,  $\text{Na}^+$  and  $\text{NH}_4^+$  is performed considering 24 cloud samples. This first analysis shows that 18 samples are of marine origin and 6 samples are classified as continental. The same statistical approach is used adding trace metal concentration. Zn and Mg elements are the most abundant trace metals for all clouds. A higher concentration of Cd is mainly associated to clouds from marine origins. Cu, As, Tl and Sb elements are rather found in the continental samples than in the marine ones. Mg, V, Mn and Rb elements mainly found in soil particles are also more concentrated in the samples from continental air mass. This new PCA including trace metal confirms the classification between marine and continental air masses but also indicates that one sample presenting low pH and high concentrations of  $\text{SO}_4^{2-}$ , Fe, Pb and Cu could be rather attributed to a polluted event.

**Keywords:** cloud; trace metals; puy de Dôme; principal component analysis; air mass origin

## 1. Introduction

Clouds contain a myriad of inorganic and organic compounds resulting from the dissolution of aerosol particles acting as Cloud Condensation Nuclei (CCN) and from the mass transfer of chemical species from the gas to the aqueous phase depending on their solubility. Among these compounds, trace metal elements are present in atmospheric waters (rain, snow, fog and cloud droplets) in low concentration (from  $\text{mg}$  to  $\mu\text{g L}^{-1}$ ) and result essentially from particle dissolution. The dissolution of particles into liquid phase after nucleation depends on several factors: the solubility of trace metals is

accelerated when the acidity increases; the nature of the solid matrix governs the kinetic of dissolution; finally, it was demonstrated that dissolution is photochemically initiated [1–5]. Determining the concentrations of these trace elements is of ecological interest due to their toxicity as pollutants [6,7]. They have sanitary impact: for example, high concentration of Zn is proved to have health effects; As, Cd and Pb are considered as carcinogenic while the inhalation of Mn can cause psychiatric and movement disorders, respiratory effects and reproductive dysfunction [8]. Moreover, trace metals, like Cu, Mg, Mn and Zn, are key compounds for biological activity since they constitute the active center of many enzymes [9]. Despite this, anthropogenic emissions are the dominant atmospheric sources in comparison to trace metals solely involved in biological activity [10].

Trace metals can originate from crustal dust or from aerosols resulting either from marine or anthropogenic sources [11,12]. Trace elements, like As, Cr, Cd, Co, Tl, V and Sb are emitted as particulate components by vehicles exhausts, road dust, coal and oil combustion, fly ashes from wood combustion, refuse incineration, and widespread industrial use [13]. In case of a crustal origin, compounds such as carbonates, oxides, sulfides, and silicates are characterized by low solubility, except for low pH values. Elements associated with marine and anthropogenic sources are more soluble [14]. Cloud water droplets contain dissolved metals but also insoluble metal particles, with an average median diameter between 50 to 250 nm [15]. Ghauri et al. [16] filtered cloud water samples through 0.45  $\mu\text{m}$  filters and performed trace metal analysis on the filtrate and the filter (particles > 0.45  $\mu\text{m}$ ). They then estimated that the solubility of As, Sb, Cd and Pb, (elements associated to anthropogenic sources), was very high (90%), while the solubility of Cu and Mn, (elements related to both anthropogenic and natural sources), was estimated to be 80–90%. Crustal elements like Al and Ti showed intermediate results (45%). Fe is the most concentrated transition metal (from 0.05 to 50  $\mu\text{g L}^{-1}$  in rain drops and from 0.05 to 50  $\text{mg L}^{-1}$  in cloud droplets), but its solubility is mainly dependent on the particle origin. On the one hand, anthropogenic particles, where Fe is adsorbed onto carbonaceous matter tends to have high solubility, while, on the other hand, crustal dust is less soluble and mainly composed of silicate and carbonate [2]. Filtration through a fine sieve retains larger particles, generally of crustal origin, while Fe adsorbed in smaller carbonaceous particles efficiently dissolves in cloud water [17].

The redox cycle of dissolved trace metals plays an important role on cloud water reactivity. Numerous parameters such as the oxidation state, the complexation and pH, influence the reactivity of transition metals. Mn, Cu and Fe are the most abundant transition metals in cloud water [1]. They catalyze the oxidation of S(IV) to S(VI) [18–20]. Besides, Fe and Cu substantially influence the hydroxyl radical budget through their reactions with hydrogen peroxide ( $\text{H}_2\text{O}_2$ ) and peroxy radicals ( $\text{HO}_2^\bullet/\text{O}_2^{\bullet-}$ ). In particular, Fe in both oxidized and reduced states triggers the formation of hydroxyl radical via the photolysis of Fe(III) and the Fenton reaction in some kind of catalytic cycle where it is regenerated [1]. These reactions are considered in cloud chemistry models [21–23], but the ability of iron to control the oxidative budget depends on the presence of carboxylate compounds that can complex the iron [24,25]. Recently, siderophore molecules, like pyoverdine, produced by microbial activity are likely to complex Fe [26,27]. These siderophores undergo phototransformation, which leads to the reduction of Fe(III) to Fe(II), influencing metals redox cycle and consequently their effect on cloud chemistry [28].

Even if in rural and continental background regions trace metal concentrations in cloud water are relatively low [13], their concentrations are dependent on the air mass origin and these can help to better discriminate cloud samples.

In this study, 24 cloud water samples were collected at the puy de Dôme station (France) (PUY). Air masses sampled at this site have contrasted chemical composition and are representative of various geographical origins [29,30], resulting from mixed contribution of marine and/or continental influence. The concentrations of 18 elements were analyzed by ICP-MS (Inductively Coupled Plasma Mass Spectrometry). Clouds are classified based upon the main anions and cations concentrations using principal components analysis (PCA) following the work from Deguillaume et al. [31]. Here,

trace metal concentrations are added to this statistical analysis with the objective to better discriminate cloud samples among continental and marine origins.

## 2. Materials and Methods

### 2.1. Cloud Water Sampling and Physico-Chemical Parameters

Cloud water samples are collected at the top of puy de Dôme Mountain (45.5° N, 2.75° E; 1465 m a.s.l.) in France. The observatory (PUY) is part of the atmospheric survey networks EMEP (the European Monitoring and Evaluation Programme), GAW (Global Atmosphere Watch), and ACTRIS (Aerosols, Clouds, and Trace gases Research Infrastructure). Cloud water microphysical parameters, like liquid water content (LWC) and effective droplet radius, are measured continuously by a Particulate Volume Monitor (PVM Gerber 100U). The samples were collected for contrasted seasons and two different years: in March, April and November 2014 and February and June 2016. During these periods, the site has been shown to be mainly located in the free troposphere [30,32,33]. Thus, the station was not influenced by local emissions. The air mass origin for each event is calculated using 72 h back-trajectories obtained by the NOAA HYSPLIT (Hybrid Single Particle Lagrangian Integrated Trajectory Model) Trajectory Model (Figure 1) using GDAS (Global Data Assimilation System) (1 degree, global, 2006–present) archive.

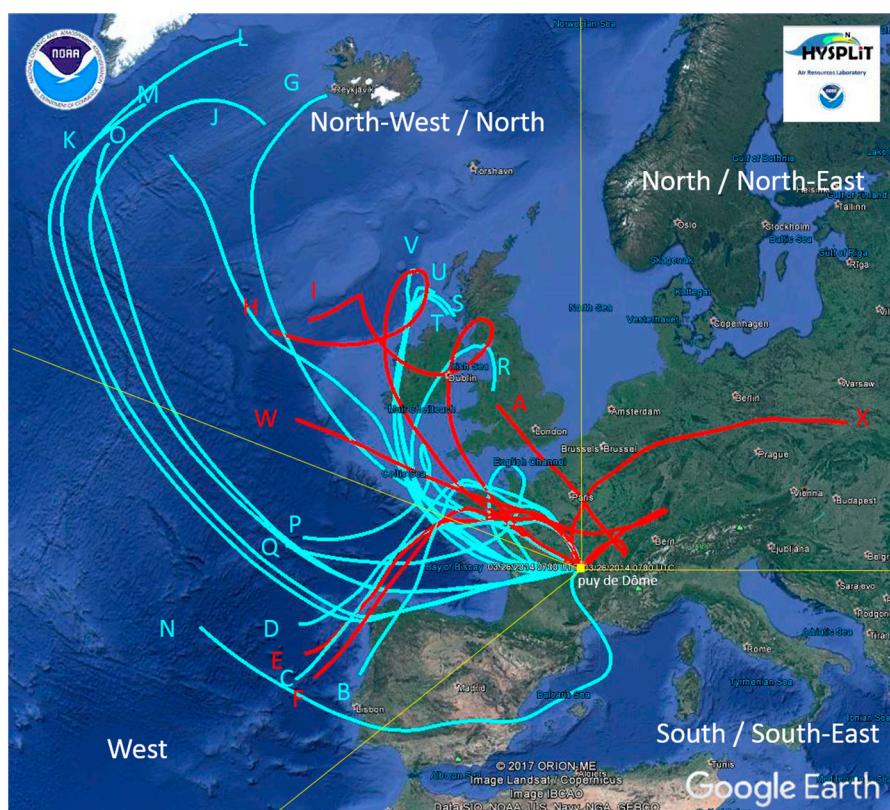


**Figure 1.** Back-trajectory sectors of air masses reaching the puy de Dôme. Yellow lines depict the four different sectors identified: Air mass origin was calculated by NOAA-HYSPLIT using 72 h back-trajectory and the direction of air mass before arriving at the puy de Dôme mountain is reported in blue for marine samples and in red for continental samples, following the HCA1 (hierarchic cluster analysis) analysis performed on samples analyzed in this work plus samples from Deguillaume et al. [31] (174 observations).

The cloud water sampling is performed with a dynamic one stage cloud water impactor, for which the cut-off diameter is approximately  $7\ \mu\text{m}$  [34]. The homemade impactor is of aluminum and sterilized by autoclave before using. Cloud droplets are collected by impaction onto a rectangular aluminum plate. Samples are collected in sterilized bottles and cloud water is filtered using a  $0.2\ \mu\text{m}$  nylon filter within 10 min after sampling to eliminate microorganisms and larger particles. The dataset is composed of 22 samples, corresponding to eight cloud events, collected during two campaigns (26 March to 5 April 2014, 5 November to 19 November 2014) and 2 individual samples collected in February and June 2016. Those samples are representative of the conditions encountered at the puy de Dôme, which, most of the time, are marine (52%) and continental (26%). More precisely, those samples represent a significant fraction of the clouds reaching the top of the puy de Dôme Mountain [31], where clouds result from air masses, coming from the west, north/west sectors (72% of occurrence).

Samples are characterized by pH measurement immediately after sampling while ion chromatography (IC) and ICP-MS (Inductively Coupled Plasma Mass Spectrometry) are performed on frozen samples. IC analysis is performed using a DIONEX DX-320 equipped with an IonPac AG11 (guard-column  $4 \times 50\ \text{mm}$ ) and an IonPac AS11 (analytical column  $5 \times 250\ \text{mm}$ ) for anions, a DIONEX ICS-1500 equipped with an IonPac CG16 (guard-column  $4 \times 50\ \text{mm}$ ) and an IonPac CS16 (analytical column  $5 \times 250\ \text{mm}$ ) for cations.

### 2.2. ICP-MS (Inductively Coupled Plasma Mass Spectrometry) Analysis

Aliquots of  $500\ \mu\text{L}$  of cloud water samples are directly transferred in  $6\ \text{mL}$  ICP-MS polystyrene vials previously conditioned by immersion for 24 h in diluted nitric acid followed by repeatedly washes with ultrapure (Milli-Q) water. Samples are diluted with  $4500\ \mu\text{L}$  of distilled  $\text{HNO}_3$  1 M in MilliQ water. Trace elements abundances are determined by ICP-MS (Agilent 7500). Sample solutions are aspirated at a rate of  $400\ \mu\text{L}/\text{min}$  using a peristaltic pump and introduced into the plasma using a quartz introduction system (Micromist Nebulizer and a Scott-type spray chamber). The analyses are performed in plasma robust mode (1550 W). The instrument is tuned so that the mass interferences of oxides and doubly charged ions (as monitored from CeO and  $\text{Ce}^{2+}$  respectively) do not exceed 1%, and thus can be neglected for most elements. The Helium collision cell of the ICP-MS is used to reduce interferences on the signals from 25 Mg to 77 Se masses. The signal is calibrated externally with multi-element standards (1 and  $10\ \text{ng g}^{-1}$ ), which are prepared by gravimetric dilution of  $10\ \mu\text{g mL}^{-1}$  certified solutions traceable to NIST (National Institute of Standards and Technology) (Inorganic Ventures). Concentrations values in  $\mu\text{g g}^{-1}$  are converted in  $\mu\text{g L}^{-1}$  considering the solution density ( $1.01\ \text{kg L}^{-1}$ ). Limit of quantification (LQ) is reported in Table S1, and it is calculated from five independent measurements of the signal acquired on the MilliQ- $\text{HNO}_3$  redistilled. On the average the LQ ranges from  $0.01$  to  $4.2\ \mu\text{g L}^{-1}$  for more concentrated elements (Mg, Ti, Fe, Cu, Zn, Sr) to  $1$  to  $60\ \text{ng L}^{-1}$  for less concentrated elements (V, Mn, Co, As, Rb, Cd, Sb, W, Tl, Pb, U). Li, Be, Sc, Cr, Ga, Se, Nb, Pd, Ag, Mo, In, Sn, Te, Ta, Pt and Bi are measured for each sample, but their concentrations are below the LQ. The experimental blank is executed spreading Milli-Q water on the cloud water impactor and collecting it in clean Falcon<sup>®</sup> tube (the same used for samples). Blank is treated as a sample and results are reported in Table S1. The cloud water collector is constituted by aluminum, thus this element is not measured in the samples.

### 2.3. PCA (Principal Component Analysis) and HCA (Hierarchic Cluster Analysis)

An unsupervised multivariate statistical approach is used: PCA loadings are calculated as linear combinations of the variables (i.e., physicochemical parameters); the first two factorial axes, called Dimension 1 and Dimension 2, are uncorrelated between themselves and report the variability of the matrix. The PCA is performed with XStat, an add-in package of Microsoft Excel [35]. The data matrix is automatically standardized by the software and the Pearson correlation coefficient is used. The number of factorial axes retained for the analysis is of two for each case presented: this limits the robustness of the PCA analysis, but it allows a better visual representation and comparison

to the data presented in the previous classification by Deguillaume et al. [31]. The combined plot of scores (coordinates of the samples on the new variables) and loadings (weights of original variables on Dimension 1 and Dimension 2) called bi-plot allows us to identify groups of samples with similar behavior and the existing correlation among the original variables. PCA is performed considering the concentrations in micromolar ( $\mu\text{M}$ ) in order to classify cloud samples using the same approach of Deguillaume et al. [31] (6 variables) (Figure S1). For samples presenting concentrations below the detection limit, concentration values were considered equal to 0 in the statistical analysis. For the statistical study considering the total trace metal concentration or the individual trace metal concentrations, all the concentrations (ions, pH and metal) are in  $\mu\text{g L}^{-1}$ . In the present work, Hierarchic Cluster Analysis (HCA), using Euclidean square distance and Ward method was used on reduced and centered data to assign samples to the classes defined by Deguillaume et al. [31]: “marine”, “highly marine”, “continental” and “polluted”. Back-trajectory plots are calculated to confirm the statistical classification.

### 3. Results and Discussion

#### 3.1. Sample Characteristics

Table S2 reports 24 individual samples, corresponding to 10 cloud events, characteristics: sampling period, pH, main ions and cations' concentrations ( $\text{mg L}^{-1}$ ) and trace element concentrations ( $\text{mg L}^{-1}$  for Mg and  $\mu\text{g L}^{-1}$  for other metals). The metal concentrations are very low and most of the time they are below the limit of quantification (LQ). This could be explained by the remoteness of the puy de Dôme site from local sources [31,36]. Figure 2a reports the distribution of trace metal concentrations in a box plot. The median concentration is significantly different from zero for most of the trace metals except for Mn, Fe, Co, Tl, Pb and U, which are not present in all the samples and which show a value of 0 for the median of concentration. Co, Tl, Pb and U are present in 25–45% of samples and in extremely low concentration, except for Pb. Fe presents the higher LQ of  $1.42 \mu\text{g L}^{-1}$ : this is probably due to the ubiquitous presence of this element and to the contamination risk and its low concentration not being significant compared to a high LQ value. Most of the samples present a concentration below the detection limit except two samples (H and I) with a high level of Fe. Mn is present in 45% of the samples with an average concentration of  $2.34 \mu\text{g L}^{-1}$ : Its concentration is highly variable. The most concentrated elements are Mg and Zn, and results are reported in  $\text{mg L}^{-1}$  in red in the box plot in Figure 2a.

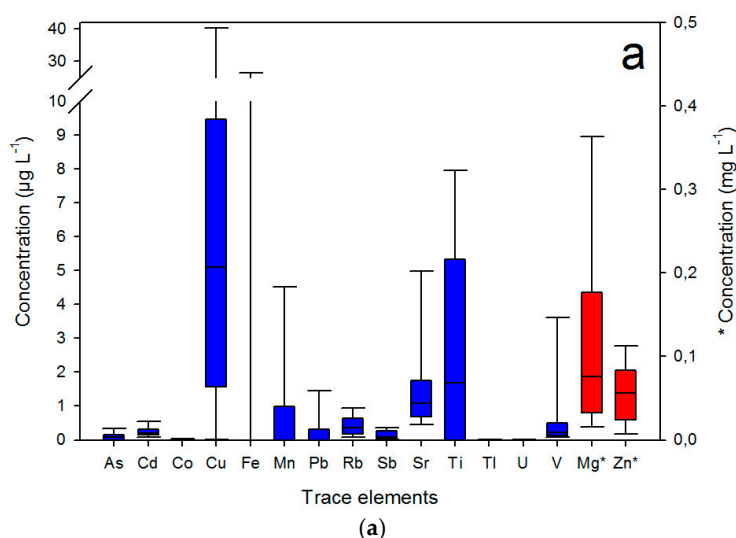
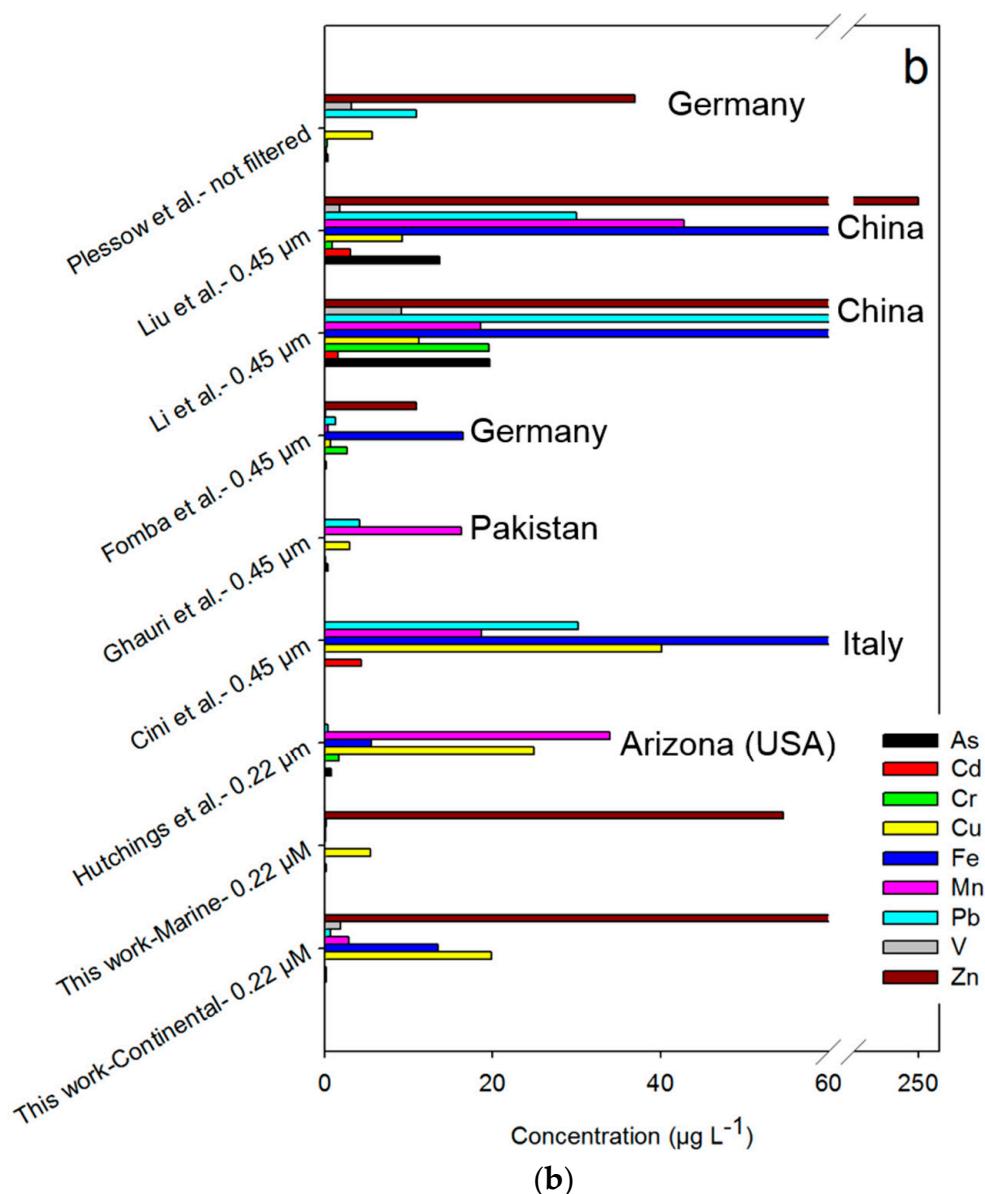


Figure 2. Cont.



**Figure 2.** (a) Box-plot showing concentration of trace metals in this work. The boundary of the box closest to zero indicates the 25th percentile, a line within the box marks the median, and the boundary of the box farthest from zero indicates the 75th percentile. Whiskers above and under the box indicate the 90th and 10th percentiles. Mg and Zn are reported in  $\text{mg L}^{-1}$  in red (right axis); (b) Comparison between data reported in this work and from other sites. (Hutchings et al. [37]: filtered  $0.22 \mu\text{m}$ ; Cini et al. [13]: filtered  $0.4 \mu\text{m}$ ; Ghauri et al. [16]: filtered  $0.45 \mu\text{m}$ ; Fomba et al. [13]: filtered  $0.45 \mu\text{m}$ ; Li et al. [15]: filtered  $0.45 \mu\text{m}$ ; Liu et al. [38]: filtered  $0.45 \mu\text{m}$ ; Plessow et al. [5]: not filtered.); (Site characteristics are reported in Table S2.).

The same range of concentrations has been observed at Mt. Brocken, a remote sampling site in Germany by Plessow et al. [5] ( $\text{Mg } 115 \mu\text{g L}^{-1}$ ,  $\text{Zn } 37 \mu\text{g L}^{-1}$ ). In our case, Mg has an average concentration of  $160 \mu\text{g L}^{-1}$ ; it mainly derives from natural sources such as soil dust, under the form of silicate or carbonate, or it is emitted as sea salt, as chloride. Concerning Zn concentrations, which show an average value of  $58 \mu\text{g L}^{-1}$ , Kim and Fergusson [39] measured Zn on aerosols collected in a residential city area and estimated that natural sources (i.e., sea salt spray and mineral dusts) are the most important, followed by anthropogenic sources like tire wear, coal combustion and traffic emissions. A great contribution to Zn concentration in marine air masses could be the enrichment of the

sea-surface microlayer with Zn and the effect of metal scavenging by bubble bursting [40,41]. The ratio of Zn to Sb for cloud samples collected at Mt. Plynlimon (United Kingdom) between 1992 and 1995 depends on air mass origin. This is due to the fact that Zn is mainly emitted by natural sources while Sb is released into atmosphere by anthropogenic sources such as industries, combustion processes or automobile exhausts [42]. Wilkinson et al. [6] found that the Zn content is highly correlated with the marine content leading to a high Zn/Sb ratio. They fixed a threshold value for the Zn/Sb ratio at 80 to discriminate between marine air masses (>80) and polluted air masses. In our samples, the average Zn/Sb ratio is  $780 \pm 1000$  and the minimum value is 80.9 (sample O), indicating that cloud water samples collected at the puy de Dôme station were not affected by anthropogenic pollution along their trajectory. This result supports the general assumption of remoteness of the site in agreement with other results obtained in this work and in previous studies [31,43].

Figure 2b displays the concentrations of trace metals at the PUY compared to cloud water data from previous studies. Concentration of trace metals reported in our work is usually lower than previous results. This can be explained by several reasons. The first sensitive parameter is sample filtration: in this study cloud waters were filtered with 0.22  $\mu\text{m}$  Nuclepore filter and particulate trace metals are considered to be retained by the filter. As reported in the introduction, filtration is a crucial step [16]: crustal dust mainly consists of particles with a mass median radius of circa 20  $\mu\text{m}$  if the average transport is <1000 km, of 5–10  $\mu\text{m}$  for medium length transport (5000 km) and of 2  $\mu\text{m}$  for longer transport [44]. Crustal dust particles are retained by the filter and metals are not soluble because they are included in silicate or carbonate crystalline lattice. For this reason, a low concentration of dissolved trace elements is expected from this source. Carbonaceous matter is associated with smaller particles 1–10  $\mu\text{m}$  with transition metals adsorbed on an organic matrix and thus more soluble [2]. Only Hutchings et al. [37] used the same filters as this study (0.22  $\mu\text{m}$ ), while the other studies used filtration through 0.45  $\mu\text{m}$  filter or, in the case of Plessow et al. [5], they did not filter the cloud samples.

The second factor that needs to be considered is the air mass origin: Hutchings et al. [37], Ghauri et al. [16], Fomba et al. [13] and Plessow et al. [5] sampled clouds at continental sites. Therefore, cloud water has a higher concentration of crustal trace elements. Cini et al. [14] reports that the Vallombrosa region (Tuscan Appennines, Italy) is influenced by sea components (marine origin air masses) but also exposed to significant pollution sources [14]: this observation can explain the high trace metals concentration found in comparison to this work and to other studies. References [15,38] collected samples in a continental region in China characterized by high emissions of pollutants. Mt. Lu, in Jiangxi province (south-east of China), is influenced by emissions of fine metals particles from large, non-ferrous industries and coal-fired power, while Mt. Tai, in Shandong province (northern China Plain), is affected by emissions of mining activities and steel industries. These sites are thus considered as polluted.

Results for the puy de Dôme site are reported, but a discrimination has been made following the same procedure as Deguillaume et al. [31] for the 24 cloud samples separated into two classes: continental and marine (see Section 2.2). Arsenic (As) concentrations in cloud waters collected at the puy de Dôme site from marine and continental origins are low and are comparable to those reported for References [5,13,14,16,37] (marine and continental sites), whereas References [15,38] which are related to polluted sampling sites, show concentrations 15–20 times higher. Cd concentrations are close to those reported by References [5,16], but lower than those reported by other works. In addition, there is no significant difference between marine and continental air masses. Cr, a typical marker of pollution, is not present in our samples and is reported to be below the detection limit as in References [14,16], while it is measured for the other works, in particular for References [15,38] in China. Regarding Cu, concentrations from continental air masses are comparable to References [14,37] and are larger than marine Cu concentrations. However, marine Cu concentrations at the PUY are in the same range as for the ones in References [5,13,15,16,38]. Mn and Fe in both continental and marine origin samples presented in this work show low concentrations: this is probably due to the fact that these trace metals are mostly insoluble when they come from crustal particles, while they are more soluble if adsorbed

in carbonaceous aerosol, associated with anthropogenic emissions. Vanadium (V) in continental air masses shows similar concentration to References [5,38] while, in marine samples, its concentration is lower, compared to Reference [13]. Zn presents concentrations comparable with References [5,13], but lower than concentrations measured at polluted sites [15,38].

### 3.2. Principal Components Analysis (PCA)

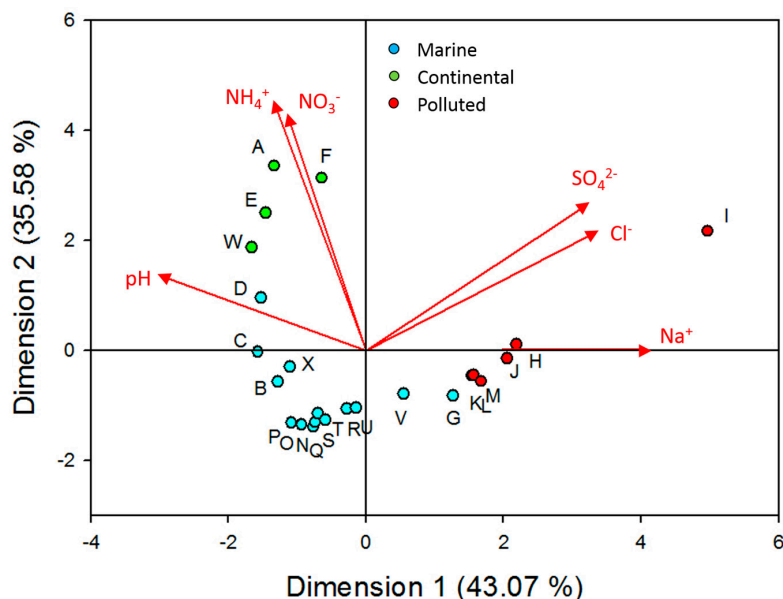
Deguillaume et al. [31] performed PCA and HCA considering physico-chemical parameters (pH) and major inorganic anions and cations concentrations ( $\mu\text{M}$ ) ( $\text{Cl}^-$ ,  $\text{NO}_3^-$ ,  $\text{SO}_4^{2-}$ ,  $\text{Na}^+$  and  $\text{NH}_4^+$ ). PCA and HCA are useful tools to classify air masses reaching the puy de Dôme summit. Four classes were identified: polluted, continental, marine and highly marine. Back-trajectory plots are used a posteriori to confirm the classification obtained by HCA. Highly marine clouds show higher concentrations of  $\text{Na}^+$  and  $\text{Cl}^-$  than the marine clouds. Air masses classified as marine and highly marine originate from west and northwest directions, as shown in Figure 1. Continental and polluted air masses have the second highest and highest level of  $\text{NO}_3^-$  and  $\text{NH}_4^+$ , respectively, and come from north and northeast directions. The presence of  $\text{SO}_4^{2-}$  is related to polluted air masses. Air masses coming from the south and southeast directions show mainly marine characteristics.

Figure S1 shows the bi-plot obtained by PCA for physicochemical parameters considering samples analyzed in this work (yellow triangles) plus other samples from the database of the puy de Dôme station [45] (circles) (PCA1). As expected, the samples fall into four classes: polluted (red circles), continental (green circles), marine (light blue circles) and highly marine (blue circles). The PCA variables are represented by red arrows and the correlation between  $\text{Na}^+$  and  $\text{Cl}^-$  and between  $\text{SO}_4^{2-}$ ,  $\text{NO}_3^-$  and  $\text{NH}_4^+$  is clear. HCA1 (Figure S2) allows for classifying cloud waters presented in this work: six samples are assigned to the continental class (A, E, F, H, I and W), while the rest of the samples (18) are attributed to the marine class. None of the cloud sampled was from highly marine or polluted origins. Results are reported in Table S2 along with data sampling parameters and chemical concentrations. Even if a neat grouping can be observed in the PCA bi-plot, samples corresponding to marine and continental air masses belong to the same area of the plot. Table 1 reports the main statistical variables calculated for the cloud samples considered in this work (24 observations).

**Table 1.** Minimum (Min), first quartile (1st Qu), median, mean, third quartile (3rd Qu) and maximum (Max) values for samples considered in this work (24 observations). Concentrations are reported in  $\mu\text{M}$  as in Deguillaume et al. [31].

Parameter	pH	$\text{Cl}^-$	$\text{Na}^+$	$\text{NO}_3^-$	$\text{SO}_4^{2-}$	$\text{NH}_4^+$
Min.	4.1	2.0	3.2	6.1	8.0	0.0
1st Qu.	5.3	7.9	10.6	19.9	15.8	0.0
Median	5.5	22.3	17.9	22.9	25.1	1.1
Mean	5.5	33.0	30.5	53.9	40.4	51.9
3rd Qu.	5.7	52.6	45.7	53.0	38.6	87.5
Max.	6.9	98.0	99.0	224.1	247.4	252.4

The same approach used by Deguillaume et al. [31] is applied to the dataset composed of the 24 samples presented in this work, and Figure 3 reports the bi-plot obtained (PCA2). HCA2 (Figure S3) leads to a different classification of cloud water samples: four samples (A, E, F and W) are classified as continental, 14 samples as marine and six samples (H, I, J, K, L and M) are attributed to the polluted class. The classification obtained by HCA2 on the reduced sample set (24 samples) is different from the one obtained by HCA1 for the whole sample set (174 samples).



**Figure 3.** Bi-plot resulting from the PCA (principal component analysis) (PCA2) and detailing: with circles, the scores of the samples presented in this work (marine in light blue, continental in green, polluted in red); with the red vectors, the loadings of the six experimental variables pH, Cl<sup>-</sup>, NO<sub>3</sub><sup>-</sup>, SO<sub>4</sub><sup>2-</sup>, Na<sup>+</sup> and NH<sub>4</sub><sup>+</sup>; (PCA is performed using  $\mu\text{M}$  unit concentrations and automatic normalization of the data).

To solve the ambiguity of the two PCA/HCA results and to refine the air mass origin, trace metal concentrations are added to the PCA analysis. As a first step, the total trace metal concentration, calculated as the sum of single metal concentrations in a sample, has been added to the PCA analysis (PCA3). All the concentrations in this analysis are expressed in  $\mu\text{g L}^{-1}$ . No correlation is found between total trace metal concentration and other variables, as shown in the correlation matrix (Table S4), which presents low correlation factor (from 0.1 to 0.3). SO<sub>4</sub><sup>2-</sup> is not correlated to NO<sub>3</sub><sup>-</sup> and NH<sub>4</sub><sup>+</sup> for the 24 selected samples, but it is slightly correlated to Na<sup>+</sup> and Cl<sup>-</sup>. This result is due to the dual origin of sulfates, from oxidation of SO<sub>2</sub> (continental and polluted air masses) and from sea salt spray (marine air masses). It indicates that the concentration of sulfates for the analyzed samples is mostly correlated to the sea salt dissolution in cloud droplets, but in some cases is related to the anthropogenic sources. Therefore, samples B, C, D, E and from J to X show the same concentrations even if they are associated with marine or continental origin air masses. Trace metals are attributed to different sources and, for this reason, the sum of the concentration of each single metal is correlated to natural and anthropogenic contributions, and it is not suitable to use this parameter to discriminate between marine and continental origins.

Thereby, in a second step, the PCA (PCA4) is performed using the physicochemical parameters and the concentration of each individual metal as variables. Titanium (Ti) and Copper (Cu) concentrations, which are similar for the whole samples, are not considered in the PCA study, as well as Uranium (U) for which the concentration is near or below the LQ for all the samples. The bi-plot is reported in Figure 4 and shows that marine samples are located in the second and third quadrant of the Cartesian space while continental samples are grouped in the fourth quadrant.

The first quadrant contains only two samples that will be analyzed in detail in the following. The similarity of the 24 samples presented in this work makes it difficult to compel the PCA analysis that cannot be considered as a robust statistical approach in this case. Anyway, some correlation between variables can be investigated: correlation coefficients, which vary between  $-1$  and  $1$  ( $-1$  anticorrelation,  $0$  no correlation,  $1$  correlation) are used for discussion and are reported in Table 2.

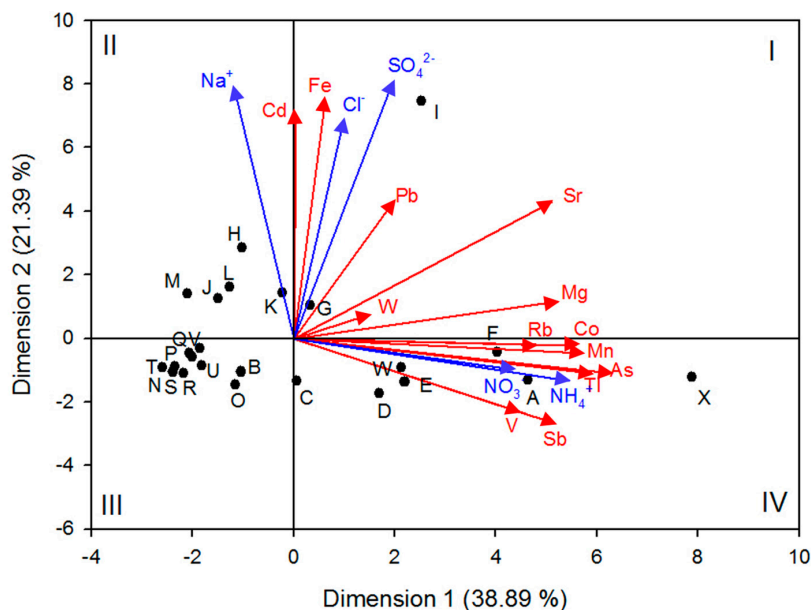


**Figure 4.** Bi-plot resulting from the PCA (PCA4) and detailing: In circles, the scores of the samples presented in this work (black with labels); the loadings of the six experimental variables  $\text{Cl}^-$ ,  $\text{NO}_3^-$ ,  $\text{SO}_4^{2-}$ ,  $\text{Na}^+$  and  $\text{NH}_4^+$  (blue vectors); the loadings of trace metals (red vectors); (I, II, III and IV indicate, respectively, 1st, 2nd, 3rd and 4th quadrants of the Cartesian space.); (PCA is performed using  $\mu\text{g L}^{-1}$  unit concentrations and automatic normalization of the data).

Considering the physico-chemical parameters,  $\text{Na}^+$  and  $\text{Cl}^-$  are correlated, as described by the correlation coefficient of 0.83, as well as  $\text{NH}_4^+$  and  $\text{NO}_3^-$ , which present a value of 0.85.  $\text{Na}^+$  is anticorrelated with  $\text{NH}_4^+$  and  $\text{NO}_3^-$ , and their vectors allow identifying marine and continental samples.  $\text{SO}_4^{2-}$ , which could be associated to marine and continental origin air masses, is poorly correlated with  $\text{Na}^+$  and  $\text{Cl}^-$ , and its vector is in the first quadrant. Red vectors reported in Figure 4 show the correlation between trace elements and  $\text{Na}^+$ ,  $\text{Cl}^-$ ,  $\text{NH}_4^+$  and  $\text{NO}_3^-$ , and so to air mass origin.

Regarding trace metals, several correlations are identified along with physico-chemical parameters. First, two elements (Cd and Fe) are represented by vectors associated with marine origin air masses. Cd is considered as a marker of industrial activity: its flux in the atmosphere varies from  $0.05 \text{ ng cm}^{-2} \text{ month}^{-1}$  in Greenland to circa  $1000 \text{ ng cm}^{-2} \text{ month}^{-1}$  in the vicinity of major industrial sources [46]. Nevertheless, the ultimate receptacle of Cd is the ocean, and, paradoxically, Cd behaves as a nutrient in the ocean and its cycling and fate is intimately tied to uptake by photosynthetic microbes, their death, sinking and remineralization inside the ocean [47]. The average concentration of Cd in aerosol sampled at the puy de Dôme station was estimated to  $15 \text{ ng m}^{-3}$  by Vlastelic et al. [43], which is consistent with the observations of Cullen and Malonado [47] for rural sites. Samples presented in this work show a concentration of Cd 15 to 20 times lower than the concentration found in the cloud of continental/polluted origins [14,15], and, thereby, natural sources, such as marine aerosol and crustal dust, can be considered as main sources of Cd. The Cd concentration is in the same range ( $0.23 \pm 0.14$ ) for all the samples of marine and continental origin and only sample I shows higher concentration. Fe seem to be strictly correlated to  $\text{SO}_4^{2-}$ , but this is only an artefact of the PCA approach: Fe concentration is higher than  $50 \mu\text{g L}^{-1}$  only in two samples, which presents high  $\text{SO}_4^{2-}$  concentration, but it is below the LQ for all of the other samples. For this reason, it is difficult to attribute an origin to Fe dissolved in our samples collected at the puy de Dôme station. Deguillaume et al. [31] have shown that concentrations of iron in cloud waters sampled at the same site are significantly higher for polluted air masses. This demonstrates that iron comes mainly from the dissolution of anthropogenic particles.

**Table 2.** Correlation matrix obtained by the PCA4 (principal component analysis) analysis (24 samples) considering the concentration of  $\text{Cl}^-$ ,  $\text{NO}_3^-$ ,  $\text{SO}_4^{2-}$ ,  $\text{Na}^+$  and  $\text{NH}_4^+$  and the concentration of each single metal. The color code depicts in blue values between 0 and 0.2, in light blue values between 0.2 and 0.4, in light orange values between 0.4 and 0.6, in orange values between 0.6 and 0.8 and in dark orange values between 0.8 and 1.

Variables																		
$\text{SO}_4^{2-}$	1																	
$\text{NO}_3^-$	0.21	1																
$\text{Cl}^-$	0.60	0.09	1															
$\text{Na}^+$	0.52	-0.24	0.83	1														
$\text{NH}_4^+$	0.25	0.85	0.18	-0.30	1													
Mg	0.16	0.07	0.13	0.05	0.28	1												
V	0.02	0.32	0.14	-0.33	0.67	0.50	1											
Mn	0.11	0.51	-0.15	-0.22	0.47	0.79	0.35	1										
Fe	0.91	0.02	0.40	0.43	0.04	0.09	-0.12	0.02	1									
Co	0.14	0.15	-0.07	-0.18	0.40	0.94	0.54	0.81	0.07	1								
As	0.11	0.66	0.10	-0.17	0.78	0.68	0.58	0.76	-0.11	0.72	1							
Rb	0.13	0.33	0.15	-0.06	0.50	0.59	0.49	0.55	-0.08	0.66	0.72	1						
Sr	0.59	0.19	0.40	0.24	0.42	0.82	0.47	0.64	0.42	0.77	0.58	0.52	1					
Cd	0.49	-0.19	0.51	0.68	-0.22	0.18	-0.27	-0.01	0.39	0.03	0.02	0.05	0.38	1				
Sb	-0.01	0.54	0.05	-0.30	0.74	0.42	0.61	0.47	-0.19	0.47	0.75	0.63	0.36	-0.17	1			
W	0.13	-0.06	0.01	0.05	0.04	0.20	0.08	0.15	0.21	0.23	0.13	0.36	0.14	-0.09	0.35	1		
Pb	0.57	0.57	0.13	0.18	0.22	0.00	-0.20	0.43	0.52	0.02	0.15	0.14	0.20	0.19	-0.07	0.06	1	
Tl	0.14	0.74	0.00	-0.28	0.77	0.52	0.49	0.7	-0.01	0.59	0.79	0.61	0.49	-0.01	0.64	-0.06	0.38	1

Secondly, As, Tl and Sb are well correlated to  $\text{NH}_4^+$  and  $\text{NO}_3^-$ . This means that their presence is related to continental origin air masses (emission of anthropic and crustal particles). Vlastelic et al. [43] reported that As, Tl and Sb are enriched in the aerosol samples collected at the puy de Dôme station compared to the remote Atlantic environment. These are calcophile elements that come from the dissolution of mineral dusts resulting from the alteration/removal of primary particles after a short history of transport [48,49]. Mg, V, Mn and Rb are lithophile elements that can be found as silicates in suspended mineral dust and they are correlated to  $\text{NH}_4^+$  (correlation factor from 0.3 to 0.7): this implicates their presence in continental origin samples. Calcophile and lithophile elements are associated with the emission of crustal particles and so to the continental origin air masses. Tungsten (W) is a lithophile element, but it is not correlated to the main physicochemical parameters: This is explained by the fact that its concentration is low for all of the samples.

Finally, the first quadrant of the Cartesian space holds two samples, G and I, which are similar to sample H, located in the second quadrant. These samples were collected during the same day and are characterized by a low pH (4.1–4.7) and a high concentration of  $\text{SO}_4^{2-}$ . In particular, samples H and I show concentrations of  $\text{SO}_4^{2-}$  of 13.38 and 23.75  $\text{mg L}^{-1}$ , respectively (corresponding to 140 and 247  $\mu\text{M}$ ) and medium-high concentration of  $\text{NO}_3^-$  and  $\text{Cl}^-$ . These values could be associated with a polluted origin [31]. This is also corroborated by the high concentrations of Fe, Pb, Cu and Cd: Samples H and I present high Fe concentration (53 and 55  $\text{mg L}^{-1}$ ), high Cd concentration (0.8  $\text{mg L}^{-1}$ ) and medium-high concentration of Cu and Pb. Samples G, H and I were collected on 5 November 2014 for which an atmospheric low pressure thalweg passed across Europe from United Kingdom to the Maghreb region. It was the first low pressure episode after a warm and dry period, and it could explain the relatively high concentration of inorganics in cloud water. The high particle number concentration registered at the puy de Dôme station (2059, 3193 and 2910 particles  $\text{cm}^{-3}$  for G, H and I, respectively) reinforces the occurrence of a polluted cloud.

The HCA4 (Figure S4) performed on the same dataset allows for distinguishing between three classes: samples A, D, E, F, W and X belong to the continental class, samples B, C, G, J, K, L, M, N, O, P, Q, R, S, T, U and V belong to the marine class, while samples H and I are attributed to the polluted class. No sample belongs to the highly marine class. This result is in accordance with the PCA1/HCA1 performed considering the whole dataset of cloud water samples collected at the PUY station, except for samples H and I. This sample contains cap concentration of sulfate if we consider the range of concentrations observed at PUY and trace metal concentration allows for attributing it to the polluted class. A very interesting phenomena is observed for samples G, H and I: they belong to the same event, but they are attributed to different classes because of their physicochemical characteristics. This result underlines the importance of collecting cloud for short periods (2–3 h at least) to keep evidence of the extreme variability of air mass origin on clouds.

In conclusion, trace metal concentrations are complementary parameters that improve the discrimination among cloud events.

#### 4. Conclusions

The puy de Dôme is a remote and elevated geographical site and it is part of the atmospheric survey network EMEP, GAW and ACTRIS. Cloud water has been collected since 2001 and many physico chemical parameters, like pH and inorganic ions concentrations, are measured on each cloud sample. The classification performed by PCA and HCA by Deguillaume et al. [31] for 10 years of monitoring allows for defining the discriminating factors (pH value and the concentrations of  $\text{Cl}^-$ ,  $\text{NO}_3^-$ ,  $\text{SO}_4^{2-}$ ,  $\text{Na}^+$  and  $\text{NH}_4^+$ ) for four different classes: polluted, continental, marine and highly marine.

Clouds incorporate trace metal when the cloud droplet nucleates, and their presence is very important because they participate in chemical transformations and they have a sanitary impact. Despite this, only recently (from 2014), the concentration of 33 metal elements was measured in cloud

water collected at the puy de Dôme station. Seventeen trace metals were found to be significant and were compared to concentration ranges observed for other sites.

PCA and HCA were performed using the pH value and the concentration of  $\text{Cl}^-$ ,  $\text{NO}_3^-$ ,  $\text{SO}_4^{2-}$ ,  $\text{Na}^+$  and  $\text{NH}_4^+$  on two sets of samples: the first one is composed of the dataset used by Deguillaume et al. [31] plus 24 samples presented in this work (PCA1/HCA1), and the second one on the 24 samples presented in this work (PCA2/HCA2). The results obtained by the two analyses were contrasting: marine origin was attributed to 16 samples and continental origin to 8 samples for the HCA1 while HCA2 classified four samples as polluted, 14 samples as marine and six samples as continental. This attribution could be partially erroneous due to the fact that continental and marine origin air masses remain in a near space in the PCA bi-plot.

A PCA was performed on the 24 samples presented in this work considering the physico-chemical parameters presented before, plus the sum of trace metal concentration (PCA3). This analysis is not able to distinguish between continental and marine cloud samples. PCA4/HCA4 considers inorganic ion concentrations and the concentrations of each trace metal (except Ti, Cu and U) on 24 samples. HCA4 confirms the classification between marine and continental air masses, done by Deguillaume et al. [31] but also makes evident that two samples, rich in sulfate, iron and lead, should be rather attributed to a polluted air mass.

The measurements of trace metals in cloud water are potentially a good indicator of the air mass origin. This kind of analysis should be performed over the long term and for several cloud events coming from various origins in the future; this will help to better discriminate between the various classes of clouds (marine, continental, polluted).

**Supplementary Materials:** The following are available online at [www.mdpi.com/2073-4433/8/11/225/s1](http://www.mdpi.com/2073-4433/8/11/225/s1). Figure S1: Bi-plot resulting from the PCA (PCA1) and detailing, Figure S2: Dendrogram of hierarchic cluster analysis performed on the same dataset of PCA1, Figure S3: Dendrogram of hierarchic cluster analysis performed on the same dataset of PCA2, Figure S4: Dendrogram of hierarchic cluster analysis performed on the same dataset of PCA4. Table S1: metal concentration of samples, Table S2: Physico-chemical parameters of sampled clouds, Table S3: Description of the various cloud sampling sites where trace metal concentrations were determined. **Table S4:** Correlation matrix obtained by the PCA3 analysis considering the concentration of  $\text{Cl}^-$ ,  $\text{NO}_3^-$ ,  $\text{SO}_4^{2-}$ ,  $\text{Na}^+$  and  $\text{NH}_4^+$  and the total metal concentration.

**Acknowledgments:** The authors are very grateful to the Agence Nationale de la Recherche (ANR) for its financial support through the BIOCAP project (ANR–13-BS06-0004). This work on the analysis of the cloud water chemical composition is supported by the French Ministry and CNRS-INSU. The authors acknowledge the financial support from the Regional Council of Auvergne, from the Observatoire de Physique du Globe de Clermont-Ferrand (OPGC), from the Fédération de Recherche en Environnement through the CPER Environnement founded by Région Auvergne, the French ministry, and FEDER from the European community. K. Sellegri is acknowledged for her contribution.

**Author Contributions:** A.B., L.D. and M.V. provided cloud sampling, the statistical analysis, main figures and chemical identification under the technical direction of J.-L. P. for ICP-MS analysis. A.B., L.D. and N.C. wrote the manuscript text and main figures and M.V., M.B. and J.-M. P. participated in the discussion. All authors have revised the manuscript.

**Conflicts of Interest:** The authors declare no conflict of interest.

## References

1. Deguillaume, L.; Leriche, M.; Desboeufs, K.; Mailhot, G.; George, C.; Chaumerliac, N. Transition metals in atmospheric liquid phases: Sources, reactivity, and sensitive parameters. *Chem. Rev.* **2005**, *105*, 3388–3431. [[CrossRef](#)] [[PubMed](#)]
2. Desboeufs, K.V.; Sofikitis, A.; Losno, R.; Colin, J.L.; Ausset, P. Dissolution and solubility of trace metals from natural and anthropogenic aerosol particulate matter. *Chemosphere* **2005**, *58*, 195–203. [[CrossRef](#)] [[PubMed](#)]
3. Paris, R.; Desboeufs, K.V.; Journet, E. Variability of dust iron solubility in atmospheric waters: Investigation of the role of oxalate organic complexation. *Atmos. Environ.* **2011**, *45*, 6510–6517. [[CrossRef](#)]
4. Paris, R.; Desboeufs, K.V. Effect of atmospheric organic complexation on iron-bearing dust solubility. *Atmos. Chem. Phys.* **2013**, *13*, 4895–4905. [[CrossRef](#)]

5. Plessow, K.; Acker, K.; Heinrichs, H.; Möller, D. Time study of trace elements and major ions during two cloud events at the Mt. Brocken. *Atmos. Environ.* **2001**, *35*, 367–378. [[CrossRef](#)]
6. Wilkinson, J.; Reynolds, B.; Neal, C.; Hill, S.; Neal, M.; Harrow, M. Major, minor and trace element composition of cloudwater and rainwater at Plynlimon. *Hydrol. Earth Syst. Sci.* **1997**, *1*, 557–569. [[CrossRef](#)]
7. Zhou, S.; Yuan, Q.; Li, W.; Lu, Y.; Zhang, Y.; Wang, W. Trace metals in atmospheric fine particles in one industrial urban city: Spatial variations, sources, and health implications. *J. Environ. Sci.* **2014**, *26*, 205–213. [[CrossRef](#)]
8. Schleicher, N.J.; Norra, S.; Chai, F.; Chen, Y.; Wang, S.; Cen, K.; Yu, Y.; Stüben, D. Temporal variability of trace metal mobility of urban particulate matter from Beijing—A contribution to health impact assessments of aerosols. *Atmos. Environ.* **2011**, *45*, 7248–7265. [[CrossRef](#)]
9. Sigel, H.; Sigel, A.; Dekker, M. *Metal Ions in Biological Systems*; CRC Press: New York, NY, USA, 1996; p. 848. ISBN 0-8247-9549-0.
10. Malcolm, E.G.; Keeler, G.J.; Lawson, S.T.; Sherbatskoy, T.D. Mercury and trace elements in cloud water and precipitation collected on Mt. Mansfield, Vermont. *J. Environ. Monit.* **2003**, *5*, 584. [[CrossRef](#)] [[PubMed](#)]
11. Nriagu, J.O. A global assessment of natural sources of atmospheric trace metals. *Nature* **1989**, *338*, 47–49. [[CrossRef](#)]
12. Zhang, Y.; Mahowald, N.; Scanza, R.A.; Journet, E.; Desboeufs, K.; Albani, S.; Kok, J.F.; Zhuang, G.; Chen, Y.; Cohen, D.D.; et al. Modeling the global emission, transport and deposition of trace elements associated with mineral dust. *Biogeosciences* **2015**, *12*, 5771–5792. [[CrossRef](#)]
13. Fomba, K.W.; van Pinxteren, D.; Müller, K.; Iinuma, Y.; Lee, T.; Collett, J.L.; Herrmann, H. Trace metal characterization of aerosol particles and cloud water during HCCT 2010. *Atmos. Chem. Phys.* **2015**, *15*, 8751–8765. [[CrossRef](#)]
14. Cini, R.; Prodi, F.; Santachiara, G.; Porcù, F.; Bellandi, S.; Stortini, A.; Oppo, C.; Udisti, R.; Pantani, F. Chemical characterization of cloud episodes at a ridge site in Tuscan Appennines, Italy. *Atmos. Res.* **2002**, *61*, 311–334. [[CrossRef](#)]
15. Li, W.; Wang, Y.; Collett, J.L.; Chen, J.; Zhang, X.; Wang, Z.; Wang, W. Microscopic evaluation of trace metals in cloud droplets in an acid precipitation region. *Environ. Sci. Technol.* **2013**, *47*, 4172–4180. [[CrossRef](#)] [[PubMed](#)]
16. Ghauri, B.M.; Mirza, I.M.; Richter, R.; Dutkiewicz, V.A.; Rusheed, A.; Khan, A.R.; Husain, L. Composition of aerosols and cloud water at a remote mountain site (2.8 kms) in Pakistan. *Chemosphere Glob. Chang. Sci.* **2001**, *3*, 51–63. [[CrossRef](#)]
17. Kieber, R.J.; Peake, B.; Willey, J.D.; Jacobs, B. Iron speciation and hydrogen peroxide concentrations in New Zealand rainwater. *Atmos. Environ.* **2001**, *35*, 6041–6048. [[CrossRef](#)]
18. Deguillaume, L.; Leriche, M.; Monod, A.; Chaumerliac, N. The role of transition metal ions on HO<sub>x</sub> radicals in clouds: A numerical evaluation of its impact on multiphase chemistry. *Atmos. Chem. Phys.* **2004**, *4*, 95–110. [[CrossRef](#)]
19. Harris, E.; Sinha, B.; van Pinxteren, D.; Tilgner, A.; Fomba, K.W.; Schneider, J.; Roth, A.; Gnauk, T.; Fahlbusch, B.; Mertes, S.; et al. Enhanced role of transition metal ion catalysis during in-cloud oxidation of SO<sub>2</sub>. *Science* **2013**, *340*, 727–730. [[CrossRef](#)] [[PubMed](#)]
20. Herrmann, H.; Ervens, B.; Jacobi, H.-W.; Wolke, R.; Nowacki, P.; Zellner, R. CAPRAM 2.3: A chemical aqueous phase radical mechanism for tropospheric chemistry. *J. Atmos. Chem.* **2000**, *36*, 231–284. [[CrossRef](#)]
21. Ervens, B. Modeling the processing of aerosol and trace gases in clouds and fogs. *Chem. Rev.* **2015**, *115*, 4157–4198. [[CrossRef](#)] [[PubMed](#)]
22. Mouchel-Vallon, C.; Deguillaume, L.; Monod, A.; Perroux, H.; Rose, C.; Ghigo, G.; Long, Y.; Leriche, M.; Aumont, B.; Patryl, L.; et al. CLEPS 1.0: A new protocol for cloud aqueous phase oxidation of VOC mechanisms. *Geosci. Model Dev.* **2017**, *10*, 1339–1362. [[CrossRef](#)]
23. Tilgner, A.; Bräuer, P.; Wolke, R.; Herrmann, H. Modelling multiphase chemistry in deliquescent aerosols and clouds using CAPRAM3.0i. *J. Atmos. Chem.* **2013**, *70*, 221–256. [[CrossRef](#)]
24. Long, Y.; Charbouillot, T.; Brigante, M.; Mailhot, G.; Delort, A.-M.; Chaumerliac, N.; Deguillaume, L. Evaluation of modeled cloud chemistry mechanism against laboratory irradiation experiments: The H<sub>x</sub>O<sub>y</sub>/iron/carboxylic acid chemical system. *Atmos. Environ.* **2013**, *77*, 686–695. [[CrossRef](#)]

25. Weller, C.; Tilgner, A.; Bräuer, P.; Herrmann, H. Modeling the impact of iron–carboxylate photochemistry on radical budget and carboxylate degradation in cloud droplets and particles. *Environ. Sci. Technol.* **2014**, *48*, 5652–5659. [[CrossRef](#)] [[PubMed](#)]
26. Cheize, M.; Sarthou, G.; Croot, P.L.; Bucciarelli, E.; Baudoux, A.-C.; Baker, A.R. Iron organic speciation determination in rainwater using cathodic stripping voltammetry. *Anal. Chim. Acta* **2012**, *736*, 45–54. [[CrossRef](#)] [[PubMed](#)]
27. Vinatier, V.; Wirgot, N.; Joly, M.; Sancelme, M.; Abrantes, M.; Deguillaume, L.; Delort, A.-M. Siderophores in cloud waters and potential impact on atmospheric chemistry: Production by microorganisms isolated at the Puy de Dôme station. *Environ. Sci. Technol.* **2016**, *50*, 9315–9323. [[CrossRef](#)] [[PubMed](#)]
28. Passananti, M.; Vinatier, V.; Delort, A.-M.; Mailhot, G.; Brigante, M. Siderophores in cloud waters and potential impact on atmospheric chemistry: Photoreactivity of iron complexes under sun-simulated conditions. *Environ. Sci. Technol.* **2016**, *50*, 9324–9332. [[CrossRef](#)] [[PubMed](#)]
29. Freney, E.J.; Sellegri, K.; Canonaco, F.; Boulon, J.; Hervo, M.; Weigel, R.; Pichon, J.M.; Colomb, A.; Prévôt, A.S.H.; Laj, P. Seasonal variations in aerosol particle composition at the puy-de-Dôme research station in France. *Atmos. Chem. Phys.* **2011**, *11*, 13047–13059. [[CrossRef](#)]
30. Venzac, H.; Sellegri, K.; Villani, P.; Picard, D.; Laj, P. Seasonal variation of aerosol size distributions in the free troposphere and residual layer at the puy de Dôme station, France. *Atmos. Chem. Phys.* **2009**, *9*, 1465–1478. [[CrossRef](#)]
31. Deguillaume, L.; Charbouillot, T.; Joly, M.; Väitilingom, M.; Parazols, M.; Marinoni, A.; Amato, P.; Delort, A.-M.; Vinatier, V.; Flossmann, A.; et al. Classification of clouds sampled at the puy de Dôme (France) based on 10 years of monitoring of their physicochemical properties. *Atmos. Chem. Phys.* **2014**, *14*, 1485–1506. [[CrossRef](#)]
32. Chauvigné, A. Impact radiatif des aérosols de haute altitude. Ph.D. Thesis, Université Blaise Pascal, Clermont-Ferrand, France, 2016.
33. Hervo, M. Etude des propriétés optiques et radiatives des aérosols en atmosphère réelle: Impact de l'hygroscopicité. Ph.D. Thesis, Université Blaise Pascal, Clermont-Ferrand, France, 2013.
34. Brantner, B.; Fierlinger, H.; Puxbaum, H.; Berner, A. Cloudwater chemistry in the subcooled droplet regime at Mount Sonnblick (3106 M A.S.L., Salzburg, Austria). *Water Air Soil Pollut.* **1994**, *74*, 363–384. [[CrossRef](#)]
35. *Addinsoft Xlstat*, version 2016; Data Analysis and Statistical Solution for Microsoft Excel; Addinsoft: Paris, France, 2016.
36. Putaud, J.-P.; Raes, F.; Van Dingenen, R.; Brüggemann, E.; Facchini, M.-C.; Decesari, S.; Fuzzi, S.; Gehrig, R.; Hüglin, C.; Laj, P.; et al. A European aerosol phenomenology—2: Chemical characteristics of particulate matter at kerbside, urban, rural and background sites in Europe. *Atmos. Environ.* **2004**, *38*, 2579–2595. [[CrossRef](#)]
37. Hutchings, J.W.; Robinson, M.S.; McIlwraith, H.; Kingston, J.T.; Herckes, P. The chemistry of intercepted clouds in Northern Arizona during the north american monsoon season. *Water Air Soil Pollut.* **2009**, *199*, 191–202. [[CrossRef](#)]
38. Liu, X.; Wai, K.-M.; Wang, Y.; Zhou, J.; Li, P.; Guo, J.; Xu, P.; Wang, W. Evaluation of trace elements contamination in cloud/fog water at an elevated mountain site in Northern China. *Chemosphere* **2012**, *88*, 531–541. [[CrossRef](#)] [[PubMed](#)]
39. Kim, N.D.; Fergusson, J.E. The concentrations, distribution and sources of cadmium, copper, lead and zinc in the atmosphere of an urban environment. *Sci. Total Environ.* **1994**, *144*, 179–189. [[CrossRef](#)]
40. Lion, L.W.; Leckie, J.O. The Biogeochemistry of the Air-Sea Interface. *Annu. Rev. Earth Planet. Sci.* **1981**, *9*, 449–484. [[CrossRef](#)]
41. Piotrowicz, S.R.; Duce, R.A.; Fasching, J.L.; Weisel, C.P. Bursting bubbles and their effect on the sea-to-air transport of Fe, Cu and Zn. *Mar. Chem.* **1979**, *7*, 307–324. [[CrossRef](#)]
42. Bogen, J. Trace elements in atmospheric aerosol in the heidelberg area, measured by instrumental neutron activation analysis. *Atmos. Environ.* **1973**, *7*, 1117–1125. [[CrossRef](#)]
43. Vlastelic, I.; Suchorski, K.; Sellegri, K.; Colomb, A.; Nauret, F.; Bouvier, L.; Piro, J.-L. The trace metal signature of atmospheric aerosols sampled at a European regional background site (puy de Dôme, France). *J. Atmos. Chem.* **2014**, *71*, 195–212. [[CrossRef](#)]

44. Péwé, T.L. Origin and transportation. In *Desert Dust: Origin, Characteristics, and Effect on Man*; American Association for the Advancement of Science; The Geological Society of America: Boulder, CO, USA, 1981; pp. 61–65.
45. Deguillaume, L. Mesures de la phase aqueuse du nuage du SO BEAM. Available online: <http://www.obs.univ-bpclermont.fr/SO/beam/data.php> (accessed on 15 September 2017).
46. Williams, C.R.; Harrison, R.M. Cadmium in the atmosphere. *Experientia* **1984**, *40*, 29–36. [[CrossRef](#)]
47. Cullen, J.T.; Maldonado, M.T. Biogeochemistry of Cadmium and Its Release to the Environment. In *Cadmium: From Toxicity to Essentiality*; Sigel, A., Sigel, H., Sigel, R.K., Eds.; Springer: Dordrecht, The Netherlands, 2013; Volume 11, pp. 31–62.
48. Marx, S.K.; Kamber, B.S.; McGowan, H.A. Scavenging of atmospheric trace metal pollutants by mineral dusts: Inter-regional transport of Australian trace metal pollution to New Zealand. *Atmos. Environ.* **2008**, *42*, 2460–2478. [[CrossRef](#)]
49. Moreno, T.; Querol, X.; Castillo, S.; Alastuey, A.; Cuevas, E.; Herrmann, L.; Mounkaila, M.; Elvira, J.; Gibbons, W. Geochemical variations in aeolian mineral particles from the Sahara–Sahel Dust Corridor. *Chemosphere* **2006**, *65*, 261–270. [[CrossRef](#)] [[PubMed](#)]



© 2017 by the authors. Licensee MDPI, Basel, Switzerland. This article is an open access article distributed under the terms and conditions of the Creative Commons Attribution (CC BY) license (<http://creativecommons.org/licenses/by/4.0/>).